*Inorganica Chimica Acta*, 8 (1974) 209–217



# X-Ray and White Radiation Neutron Diffraction Studies of Optically Active Potassium Antimony Tartrate, $K_2Sb_2(d\text{-}C_4H_2O_6)_2 \cdot 3H_2O$ (Tartar Emetic)

MARY E. GRESS and ROBERT A. JACOBSON

*Ames Laboratory–USAEC and Department of Chemistry Iowa State University, Ames, Iowa 50010, U.S.A.*

Received May 13, 1973

*The crystal structure of dipotassium di-μ-d-tartrato (4)-bis(antimonate(III)) trihydrate has been redetermined by three-dimensional X-ray and white radiation neutron diffraction techniques. $K_2Sb_2(d\text{-}C_4H_2O_6)_2 \cdot 3H_2O$ crystallizes in space group $C222_1$ with $a = 11.192$ (2), $b = 11.696(3)$, and $c = 25.932(5)$ Å. Full-matrix least-squares refinement of the structure using 2779 X-ray intensities resulted in a conventional discrepancy factor of 0.078. A linear programming technique was used to obtain approximate neutron structure factors from the Laue intensities. The hydrogen atom positions were located by a Fourier map calculated using the derived structure factors phased by the X-ray model.*

*In the unit cell are eight tartrato-(4)-bridged binuclear anions. The coordination of the quadridentate ligands to antimony is such that the more electronegative carboxyl oxygen atoms occupy axial positions and the hydroxyl oxygen atoms equatorial positions, with average bond lengths 2.16 and 1.99 Å, respectively. The lengthening of the axial antimony–oxygen bond correlates well with similar differences in antimony–halide compounds. The water molecules are hydrogen-bonded to each other and to carboxyl oxygen atoms and connect the antimony–tartrate anions in infinite sheets parallel to the a–b plane.*

## Introduction

Optically active potassium antimony tartrate, dipotassium di-μ-*d*-tartrato(4)-bis(antimonate(III)) trihydrate, is widely used in medicine for various parasitic diseases (as "tartar emetic"), as a mordant in dyeing, and to a limited extent, as an insecticide. Evidence for dimeric complex anions (tartrato(4)-bridged binuclear complexes) in this compound has recently been established on the basis of several X-ray structural investigations. These include the racemic salt, $K_2Sb_2(d,l\text{-}C_4H_2O_6)_2 \cdot 3H_2O$,[1] $(NH_4)_2Sb_2(d\text{-}C_4H_2O_6)_2 \cdot 3H_2O$,[2] and an incomplete structural investigation of the optically active form, $K_2Sb_2(d\text{-}C_4H_2O_6)_2 \cdot 3H_2O$.[3] In the latter study, the atom positions were located from electron density projections (from 690 film data) and with no refinement of atomic coordinates.

Previous to these studies several structural formulas had been advanced for optically active potassium antimony tartrate, the most widely accepted being the Reihlen and Hezel structure[4]

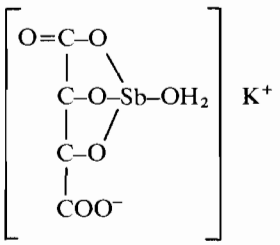


A water molecule occupying a coordination site on the antimony atom was believed to ionize in solution, thus accounting for the acidic properties of tartar emetic solutions.

Because of our interest in the coordination geometry of antimony compounds, the elongation of X-Sb-X bonds *trans* to one another and lone pair effects, if any, we have completed a more accurate X-ray structural investigation on this compound. incorporating a full-matrix least-squares refinement procedure. In addition, a neutron diffraction study using the white radiation neutron diffraction technique was undertaken to produce additional information on hydrogen atom positions and hydrogen bonding of the water molecules in the structure.

## Experimental

Single crystals of $K_2Sb_2(d\text{-}C_4H_2O_6)_2 \cdot 3H_2O$ were obtained by recrystallization of the commercially available compound from an aqueous solution. Preliminary Weissenberg and precession photographs exhibited mmm diffraction symmetry, indicating an orthorhombic space group. The systematic absences hkl when $h + k \neq 2n$ and 00l when $l \neq 2n$ uniquely determined the space

group $C222_1$. The unit cell parameters at 25°C are a = 11.192(2), b = 11.696(3), and c = 25.932(5) Å, which agree well with those found by Kiosse, Golovastikov, and Belov.[5] The unit cell parameters and their standard deviations were obtained by a least squares fit to 12 independent reflection angles whose centers were determined by left–right, top–bottom beam splitting on a previously aligned Hilger–Watts four-circle diffractometer (Cu K$\alpha$ radiation, $\lambda$ = 1.5418 Å). Any error in the instrumental zero was eliminated by centering the reflection at both $+2\Theta$ and $-2\Theta$. The calculated density (2.606 g/cc) for eight dimers per unit cell agress quite well with the observed density[6] of 2.607 g/cc.

In these studies preliminary to data collection there was a definite decomposition of the crystals which appeared to be due to loss of $H_2O$ from the crystalline lattice. Freshly prepared crystals were clear with sharply defined faces; however, the faces became less sharply defined and coated with a white powder after 2–3 days exposure to X-rays or several days exposure to the atmosphere. A neutron activation analysis for oxygen content was performed in this laboratory. The results were consistent with three water molecules per dimer for freshly prepared crystals, but showed definite water loss on exposure to the atmosphere prior to analysis.

For data collection, a crystal with approximate dimensions 0.20 × 0.20 × 0.20 mm was mounted on a glass fiber with the c axis coincident with the spindle axis and well-coated with Duco cement glue to retard decomposition. Intensity data were taken at room temperature (24°) using Zr-filtered Mo K$\alpha$ ($\lambda$ = 0.71069 Å) radiation on a fully-automated Hilger–Watts four-circle diffractometer equipped with a scintillation counter and interfaced to an SDS–910 computer in a real-time mode. 2779 intensities were measured by counting at the peak center ($\Theta_{hkl}$) for ten seconds with two five second background counts at $\Theta_{hkl} \pm (0.25 \pm (0.01 \times \Theta_{hkl}))$. For conversion of peak height to integrated data, some integrated intensities were taken by the stepscan (moving crystalmoving counter) technique[7] and a conversion table was prepared by plotting the integrated-peak height ratios as a function of theta. No dependence on *chi* or *phi* was observed.

As a general check on electronic and crystal stability, the intensities of three standard reflections were measured periodically during data collection. These reflections decreased slowly in intensity, the total decrease being 9%; such a decrease was felt to be quite acceptable and the data were appropriately corrected.

The intensity data were also corrected for Lorentz-polarization effects. The linear absorption coefficient, $\mu$, is 38.8 $cm^{-1}$. Because of the nearly spherical shape of the crystal, the transmission factor was almost a constant, 0.46–0.47, so that an absorption correction was not considered necessary. Standard deviations ($\sigma_I$) in the intensities were estimated from the total count (TC) and background count (BC) by

$$(\sigma_I)^2 = TC + BC + (0.05 \times TC)^2 + (0.05 \times BC)^2,$$

with the last two factors representing estimates for non-statistical errors in the total count and background count, respectively. Values for $\sigma_F$ were obtained by the finite difference method.[8] Of the 2779 reflections measured, the 2604 which had $F_o > 2.5\sigma_F$ were considered observed and were used in the refinement.

In order to obtain further information on the water molecule positions and on the hydrogen bonding in the solid state, neutron diffraction data were also collected.

Single crystals of $K_2Sb_2(d\text{-}C_4H_2O_6)_2 \cdot 3H_2O$ were grown by slow evaporation from an aqueous solution. A small crystal of dimensions 2.3 × 1.9 × 1.2 mm was mounted with Duco cement on a thin vanadium rod. The crystal and rod were then encapsulated in a quartz capillary, with a small piece of wetted tissue at the end of the capillary to inhibit decomposition of the crystal by loss of $H_2O$. The crystal was aligned with (110) coincident with the spindle axis by precession techniques using Mo K$\alpha$ radiation.

Neutron diffraction data were taken using the white radiation neutron diffraction technique developed in this laboratory. The experimental arrangement at the 5 M.W. Ames Laboratory Research Reactor is described elsewhere.[9,10] The intensity data were taken on a previously aligned four-circle E. and A. diffractometer interfaced to a DATEX controller and to the same SDS–910 computer as used for collection of X-ray data. The orientation of the crystal was determined by using top/bottom left/right beam splitters to tune on three reflections with $2\Theta$ fixed.

The intensities were measured at points along Laue streaks at theta values calculated from the Bragg equation $n\hat{\lambda} = 2d\sin\Theta$ in increments of $\hat{\lambda} = 0.65$ Å with $\hat{\lambda}$ initialized at 1.3 Å. (The maximum in the effective flux occurs near 1.3 Å.) Data for one octant were collected in the range $\Theta = 7.50°$ to $\Theta = 45°$. The counting period for each intensity was set by $8 \times 10^5$ monitor counts of the incident beam as detected by a $^{235}U$ fission counter. As a check on crystal, flux, and electronic stability, the intensities of three standard reflections were measured between every 20 streaks, with the maximum deviation in any standard found to be only 2%. A total of 1766 intensities were measured along 1047 Laue streaks.

Background counts for the same counting period as the intensity data were taken on each side of the Laue streak at omega offsets of ±0.75° for the first 200 data points. A smooth curve was obtained for the background (the sum of the two background measurements) as a function of $2\Theta$. The observed intensity ($I_o$) was then calculated from the peak height (PH) and the background curve (BG) by

$$I_o = PH - 0.5(BG),$$

and the standard deviation ($\sigma_I$) in the intensity was calculated by

$$\sigma_I^2 = PH + 0.25(BG) + (0.02(I_o))^2.$$

The linear attenuation coefficient was calculated from hydrogen incoherent scattering and true absorption[11] by

$$\mu(\lambda) = (0.894 + 0.025(\frac{\lambda}{1.08\ \text{Å}} - 1))\text{cm}^{-1},$$

which is adequate for the wavelength range 0.7 Å to 3.0 Å. The transmission factor may be calculated from the expansion about $\lambda_o$

$$T(\lambda) = T(\lambda_o) + \frac{\delta T}{\delta \lambda}\Big|_{\lambda_o}(\lambda - \lambda_o) + {}^1/_2 \frac{\delta^2 T}{\delta \lambda^2}\Big|_{\lambda_o}(\lambda - \lambda_o)^2 \ldots$$

The maximum and minimum transmission factors at $\lambda_o(\lambda_o = 1.08$ Å) are 90% and 81%, respectively. The effect of higher order terms, evaluated for transmission at other wavelengths, has been shown by Hubbard, Quicksall, and Jacobson[10] to be relatively small.

Due to the small size of the crystal, a large percentage of intensity data were essentially at background level. Of the 1766 measured intensities, there were only 300 $>3\sigma_I$. Although few in number, we felt they would be sufficient for computation of a Fourier map and for locating the hydrogen atoms and the orientation of hydrogen O–H bonds.

## Solution and Refinement

In order to have an independent comparison with the work of Hsiang–Ch'i Mu,[3] the antimony atom positions were determined from an unsharpened Patterson map, and the other atom positions from subsequent structure factor calculations and electron density maps. All atoms are in general positions with the exception of the potassium atoms, eight of which occupy general positions and eight occupy two fourfold sets on the twofold axes. In the electron density maps one of the three $H_2O$ oxygen atom peaks was of comparable size with the other oxygen peaks in the map, while the other two were barely distinguishable above background. The positional coordinates of these second two $H_2O$ oxygen atom positions differed from the coordinates reported by Hsiang–Ch'i Mu, with there being no observable residual electron density at the Hsiang–Ch'i Mu positions even after later refinement of the structure.

The structure was refined by a full-matrix least-squares procedure using a local modification of Busing, Martin, and Levy's OR FLS[12] with isotropic temperature factors to a conventional discrepancy factor ($R = \Sigma\|F_o| - |F_c\|/\Sigma|F_o|$) of 0.139 and a weighted discrepancy factor ($\omega R = [\Sigma\Omega(|F_o| - |F_c|)^2/\Sigma\omega|F_o|^2]^{1/2}$) of 0.187. The function minimized was $\Sigma\omega(|F_o| - |F_c|)^2$ where $\omega$ is the weight defined as $1/\sigma^2(F_o)$. The scattering factors for Sb, O, C, and $K^+$ are from the tables by Doyle and Turner.[13] The antimony and potassium scattering factors were modified by the real and imaginary parts of anomalous scattering[14] and refinement was continued with anisotropic temperature factors. The two $H_2O$ oxygen atoms which were low peaks in the electron density map were refined at half occupancy with isotropic temperature factors of 4.80 and 5.25. We interpret "half-occupancy" not as disorder, but rather that time-averaged over the period of the experiment half of these molecules were lost from the crystal.

The observed intensities by white radiation neutron diffraction are given by

$$I_n^{obs}(\Theta) = k\Sigma\Phi_{eff}(\lambda_n)T(\lambda_n)y(\lambda_n)[F_{nh}/d_{nh}^*]^2$$

where k is the scale factor, $\Phi_{eff}$ is the effective flux, T is a transmission factor, y is an extinction correction, $F_{nh}$ is the structure factor, and $\lambda_n = 2d_{nh}\sin\Theta$.[9]

Approximate structure factors were obtained by the linear programming technique discussed by Hubbard, Quicksall, and Jacobson.[10] Values for the scale factor k and flux parameters P1 (Maxwellian constant) and P2 (absorption constant) were 500, 2.55, and 0.30, respectively. The derived F's were assigned phases of structure factors calculated by using neutron scattering factors[15] and the heavy atom positional coordinates and anisotropic temperature factors from the X-ray determination. A scale factor was refined and a conventional agreement factor ($R = \Sigma\|F_o| - |F_c\|/\Sigma|F_o|$) of 0.45 was obtained.

A Fourier calculation (with grid resolution 0.17 × 0.18 × 0.20 Å) clearly revealed the tartrate hydrogen positions, hydrogen atoms of one water molecule, with the hydrogen atoms of the other two water molecules (which had been refined at partial occupancy in the X-ray study) less clearly defined. Because of the large parameter to data ratio and because of the partial occupancy of some of the water molecules, it was felt that full-matrix least-squares refinement using the neutron data would not be productive. Previous experience has shown that hydrogen atom positions taken from a Fourier map average within 0.17 Å of their correct least-squares positions. The hydrogen atom positions estimated from the Fourier map are listed in Table I.

Several least squares cycles were run, however, not varying the atom positions in the initial model to refine the flux and scale factors. Weighted agreement factors of the form

$$R_{w} = \{\Sigma_i \omega_i(I_i^{obs} - I_i^{calc})^2/\Sigma_i \omega_i(I_i^{obs})^2\}^{1/2}$$

where $\omega_i = 1/\sigma_i^2$ were $R = 0.192$ for $I_{obs} > 3\sigma_I$(300 intensities) and $R = 0.234$ for all data (1766 intensities) with final scale and flux parameters k = 7.86, P1 = 2.50, and P2 = 0.56.

Refinement of the original structure with X-ray data was continued with addition of the hydrogen atom positions with X-ray scattering factors.[16] Convergence was reached at $R = 0.078$ and $\omega R = 0.100$ with the

TABLE I. Approximate hydrogen atom positions determined by white radiation neutron diffraction[a].

| | x | y | z |
|---|---|---|---|
| H(2) | 0.4516 | 0.4375 | 0.1758 |
| H(3) | 0.3812 | 0.3359 | 0.2320 |
| H(12) | 0.1562 | 0.1359 | 0.0125 |
| H(13) | 0.0188 | 0.1172 | 0.0727 |
| H(W1a) | 0.3750 | −0.2359 | 0.0820 |
| H(W1b) | 0.2516 | −0.1875 | 0.0758 |
| H(W2a) | 0.3672 | −0.2391 | 0.1578 |
| H(W2b) | 0.2453 | −0.2641 | 0.2016 |
| H(W3a) | 0.3562 | −0.0359 | 0.1500 |
| H(W3b) | 0.4531 | 0.0531 | 0.1500 |

[a] The hydrogen atoms are labeled according to the C atom to which they are bonded. For example, H(2) is bonded to C(2).

average shift/error for the last cycle of 0.01. In a final electron density difference map, all peaks above $1.0e^-/Å^3$ (which ranged up to $3.4e^-/Å^3$) lay in concentric spheres about the antimony atoms and were probably due to termination effects in the Fourier series.

Least squares refinement of the enantiomorph ((x, y, z)→(−x, −y, −z)) yielded higher agreement factors, R = 0.080 and ωR = 0.102, which indicates that the absolute configuration is indeed that of the *d*-tartaric acid dimer.

The observed and calculated structure factors for both the X-ray and neutron investigations are available from the authors on request. The final positional and thermal parameters and standard deviations of the heavy atoms as derived from the inverse matrix of the final least squares cycle are given in Table II. Interatomic distances and their deviations were calculated using OR FFE and the variance–covariance matrix from the last least squares cycle.

## Discussion

In the unit cell of $K_2Sb_2(d\text{-}C_4H_2O_6)_2 \cdot 3H_2O$ (Figure 1) are eight antimony–tartrate dimers. The dimers are tartrato-(4)-bridged binuclear complexes in which the two antimony atoms are each coordinated to a carboxyl oxygen atom and an α-hydroxyl atom from two tartrate

TABLE II. Final heavy atom positional and thermal parameters (× $10^4$)[a].

| Atom | x | y | z | $B_{11}$ | $B_{22}$ | $B_{33}$ | $B_{12}$ | $B_{13}$ | $B_{23}$ |
|---|---|---|---|---|---|---|---|---|---|
| Sb(1) | 3788(1)[b] | 3369(1) | 487(0) | 47(1) | 27(0) | 8(0) | 1(1) | 3(0) | 2(0) |
| Sb(2) | 1272(1) | 1790(1) | 1955(0) | 54(1) | 72(1) | 14(0) | −13(1) | 14(0) | −2(0) |
| K(1) | 3664(4) | 0 | 0 | 44(3) | 42(3) | 26(1) | 0 | 0 | −12(1) |
| K(2) | 0 | 5784(5) | 2500 | 64(4) | 56(4) | 18(1) | 0 | 12(2) | 0 |
| K(3) | 3464(4) | 634(4) | 3938(2) | 77(3) | 56(3) | 22(1) | −30(3) | 1(1) | 8(1) |
| O(1) | 4989(9) | 2496(8) | 988(4) | 29(6) | 43(6) | 15(2) | 7(6) | 3(3) | 2(3) |
| O(2) | 3396(10) | 4083(9) | 1165(4) | 50(8) | 39(7) | 12(2) | 24(6) | −5(3) | −4(2) |
| O(3) | 5679(9) | 2420(10) | 1791(5) | 31(7) | 60(8) | 16(2) | 8(6) | −6(3) | −5(3) |
| O(4) | 3024(10) | 2156(10) | 1943(5) | 39(7) | 48(7) | 16(2) | −1(6) | 11(3) | 0(3) |
| O(5) | 1221(11) | 3585(13) | 2059(5) | 59(9) | 90(11) | 18(2) | 16(10) | 6(4) | −8(4) |
| O(6) | 2393(13) | 5086(14) | 2180(7) | 75(11) | 67(10) | 28(3) | 18(10) | 8(5) | −12(5) |
| O(11) | 1969(10) | 3938(9) | 339(5) | 61(9) | 30(6) | 17(2) | 19(7) | −7(4) | 2(3) |
| O(12) | 2879(9) | 1926(8) | 528(4) | 41(7) | 28(5) | 12(1) | 4(5) | −2(3) | 4(2) |
| O(13) | 134(13) | 3277(11) | 162(7) | 95(13) | 62(10) | 33(4) | 29(11) | −34(6) | −9(5) |
| O(14) | 794(12) | 2232(12) | 1244(5) | 68(10) | 66(10) | 16(2) | 7(8) | 9(4) | 5(4) |
| O(15) | 1855(13) | 3075(11) | 1491(5) | 93(12) | 71(10) | 12(2) | −22(10) | 2(4) | 8(4) |
| O(16) | 1689(14) | −407(10) | 714(5) | 98(13) | 41(8) | 17(2) | −10(8) | 1(4) | −5(3) |
| C(1) | 5011(12) | 2816(11) | 1452(5) | 33(8) | 32(8) | 11(2) | −1(7) | 4(3) | 1(3) |
| C(2) | 4103(13) | 3768(12) | 1583(5) | 41(9) | 36(8) | 11(2) | −12(7) | 3(3) | 4(3) |
| C(3) | 3312(13) | 3283(11) | 2039(4) | 57(10) | 37(8) | 6(1) | 27(8) | 2(3) | 2(3) |
| C(4) | 2275(16) | 4090(15) | 2095(6) | 61(13) | 69(13) | 9(2) | 16(10) | 5(4) | −3(4) |
| C(11) | 1237(16) | 3148(12) | 286(6) | 76(14) | 37(9) | 14(2) | 27(11) | −16(5) | −5(3) |
| C(12) | 1624(12) | 1924(11) | 396(5) | 44(9) | 33(8) | 8(2) | 19(7) | 0(3) | −1(3) |
| C(13) | 912(12) | 1433(14) | 853(8) | 24(9) | 51(11) | 23(3) | −4(8) | 5(4) | 6(5) |
| C(14) | 1561(15) | 349(13) | 1031(10) | 43(11) | 33(10) | 30(5) | −13(8) | 8(6) | −3(5) |
| O(W1) | 2948(12) | −2563(14) | 747(7) | 53(10) | 79(12) | 28(3) | 9(9) | 10(5) | 6(5) |
| O(W2) | 3291(31) | −2421(29) | 1854(12) | 4.8(6) | | | | | |
| O(W3) | 4441(30) | −191(32) | 1393(12) | 5.3(6) | | | | | |

[a] The $B_{ij}$ are defined by: $T = \exp[-(h^2B_{11} + k^2B_{22} + l^2B_{33} + 2hkB_{12} + 2hlB_{13} + 2klB_{23})]$. For O(W2) and O(W3), only the isotropic temperature factors are given (under $B_{11}$). [b] In this and succeeding tables, estimated standard deviations are given in parentheses for the least significant figures.

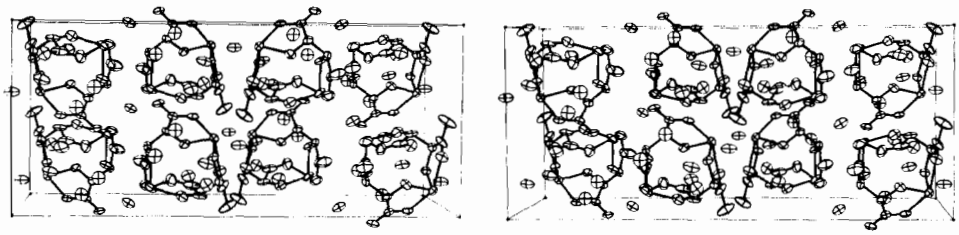

Figure 1. A stereo view of the $K_2Sb_2(d\text{-}C_4H_2O_6)_2 \cdot 3H_2O$ cell. It is viewed looking down the b axis with a up and c across the page.

groups. Racemic potassium antimony tartrate, $K_2Sb_2(d,l\text{-}C_4H_2O_6)_2 \cdot 3H_2O$, crystallizes in space group $Pca2_1$ and contains a mixture of $Sb_2(d\text{-}C_4H_2O_6)_2^{2-}$ and $Sb_2(l\text{-}C_4H_2O_6)_2^{2-}$ isomers, two *dd* and two *ll* groups per unit cell.[1] In a review of tartrate complexes, Tapscott, Belford and Paul[17] have shown that a *dl* dimer is unstable with respect to *dd* and *ll* dimers because of steric effects.

The tartrato-(4)-bridged binuclear complex is shown in Figures 2 and 3, where it can be seen that the complex possesses approximate $D_2$ point symmetry. The tartrate quadridentate ligands form four five-membered nearly planar rings with the two antimony atoms, with dihedral angles between tartrate ligands at the antimony atoms of 99°. The least squares planes are given in Table III.

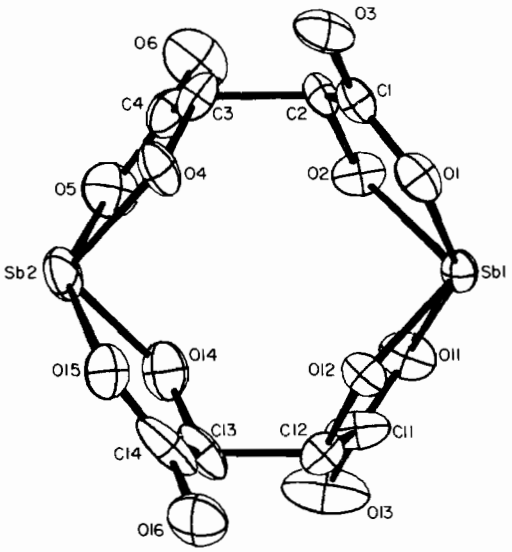


Figure 2. The $Sb_2(d\text{-}C_4H_2O_6)_2^{2-}$ anion in $K_2Sb_2(d\text{-}C_4H_2O_6)_2 \cdot 3H_2O$.

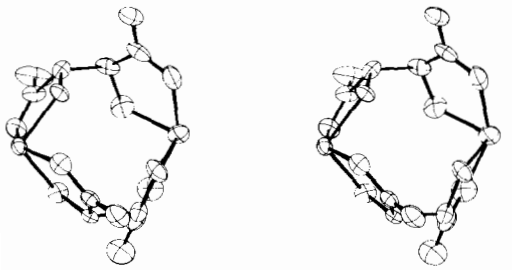

Figure 3. A stereo view of the antimony–tartrate dimer.

TABLE III. Least Squares Planes.[a]

(i) Sb(1), O(2), C(2), C(1), O(1)

| Atom | Dev.(Å) |
|---|---|
| Sb(1) | 0.029 |
| O(2) | −0.038 |
| C(2) | 0.028 |
| C(1) | 0.010 |
| O(1) | −0.028 |

Equation:
$0.6843x + 0.7010y - 0.2008z - 5.380 = 0$

(ii) Sb(1), O(12), C(12), C(11), O(11)

| Atom | Dev. (Å) |
|---|---|
| Sb(1) | −0.043 |
| O(12) | 0.047 |
| C(12) | −0.020 |
| C(11) | −0.037 |
| O(11) | 0.054 |

Equation:
$-0.1912x + 0.1239y + 0.9737z - 0.951 = 0$

(iii) Sb(2), O(15), C(14), C(13), O(14)

| Atom | Dev. (Å) |
|---|---|
| Sb(2) | −0.037 |
| O(15) | 0.035 |
| C(14) | −0.013 |
| C(13) | −0.036 |
| O(14) | 0.051 |

Equation:
$0.8871x + 0.4220y - 0.1870z - 1.235 = 0$

[a] The plane coordinates are defined relative to three orthogonal unit vectors along the a, b, and c directions.

(iv) Sb(2), O(5), C(4), C(3), O(4)

| Atom | Dev. (Å) |
|---|---|
| Sb(2) | 0.024 |
| O(5) | −0.022 |
| C(4) | 0.007 |
| C(3) | 0.024 |
| O(4) | −0.033 |

Equation:
$0.0195x - 0.1485y + 0.9887z - 4.705 = 0$

Bond distances and angles in the antimony–tartrate dimer are given in Table IV. In general, these form a very consistent set of distances and angles related by the three non-crystallographic twofold rotation axes. The carboxylic acid carbon–oxygen bond distances where oxygen is also bonded to antimony average 1.26(2) Å compared to 1.23(2) Å for carbon–uncoordinated oxygen atoms. The average C–C single bond distance is 1.54(2) Å.

The coordination of the two *d*-tartaric acid groups to the antimony atoms could be described in terms of either a distortion of a trigonal bipyramidal or a square planar bonding configuration. The axial bond angles (for two symmetry independent Sb atoms) O(1)–Sb(1)–O(11) and O(5)–Sb(2)–O(15) are 148° and 149°, and the equatorial bond angles O(2)–Sb(1)–O(12) and O(4)–Sb(2)–O(14) are 101° and 101°, respectively. Some distortion would, of course, be expected for coordination to a quadridentate ligand. Note, however, that the axial bonds are antimony–carboxyl oxygen bonds and the equatorial bonds are antimony–hydroxyl oxygen bonds. Antimony–carboxyl oxygen bond distances are 2.13, 2.18, 2.12, and 2.21 Å and antimony–hydroxyl oxygen

TABLE IV. Bond distances and angles in the antimony-tartrate dimer.

| | | | |
|---|---|---|---|
| *(a)* Distances (Å) | | | |
| Sb(1)–O(1) | 2.13(1) | Sb(2)–O(5) | 2.12(1) |
| Sb(1)–O(11) | 2.18(1) | Sb(2)–O(15) | 2.21(1) |
| Sb(1)–O(12) | 1.97(1) | Sb(2)–O(14) | 1.99(1) |
| Sb(1)–O(2) | 2.00(1) | Sb(2)–O(4) | 2.01(1) |
| C(1)–O(1) | 1.26(2) | C(11)–O(11) | 1.24(2) |
| C(1)–O(3) | 1.24(2) | C(11)–O(13) | 1.28(2) |
| C(1)–C(2) | 1.55(2) | C(11)–C(12) | 1.52(2) |
| C(2)–O(2) | 1.39(2) | C(12)–O(12) | 1.45(2) |
| C(2)–C(3) | 1.58(2) | C(12)–C(13) | 1.54(2) |
| C(3)–O(4) | 1.38(2) | C(13)–O(14) | 1.38(2) |
| C(3)–C(4) | 1.50(2) | C(13)–C(14) | 1.53(2) |
| C(4)–O(6) | 1.19(2) | C(14)–O(16) | 1.22(2) |
| C(4)–O(5) | 1.32(2) | C(14)–O(15) | 1.24(3) |
| C(2)–H(2) | 0.96 | C(12)–H(12) | 0.97 |
| C(3)–H(3) | 0.92 | C(13)–H(13) | 0.93 |
| (b) Angles (deg) | | | |
| O(1)–Sb(1)–O(11) | 147.7(4) | O(5)–Sb(2)–O(15) | 148.8(5) |
| O(2)–Sb(1)–O(12) | 101.4(4) | O(4)–Sb(2)–O(14) | 101.1(5) |
| O(11)–Sb(1)–O(12) | 77.8(4) | O(15)–Sb(2)–O(14) | 77.2(5) |
| O(1)–Sb(1)–O(2) | 78.6(4) | O(5)–Sb(2)–O(4) | 79.5(5) |
| Sb(1)–O(1)–C(1) | 116.9(8) | Sb(1)–O(11)–C(11) | 114.1(9) |
| O(1)–C(1)–O(3) | 125.2(13) | O(11)–C(11)–O(13) | 125.0(13) |
| O(3)–C(1)–C(2) | 120.5(12) | O(13)–C(11)–C(12) | 115.5(15) |
| O(1)–C(1)–C(2) | 114.3(12) | O(11)–C(11)–C(12) | 119.4(13) |
| C(1)–C(2)–O(2) | 113.2(12) | C(11)–C(12)–O(12) | 108.6(12) |
| C(2)–O(2)–Sb(1) | 116.7(8) | C(12)–O(12)–Sb(1) | 119.3(7) |
| O(2)–C(2)–C(3) | 111.0(11) | O(12)–C(12)–C(13) | 108.7(11) |
| C(2)–C(3)–O(4) | 109.8(10) | C(12)–C(13)–O(14) | 111.2(13) |
| C(3)–O(4)–Sb(2) | 115.4(9) | C(13)–O(14)–Sb(2) | 118.5(11) |
| O(4)–C(3)–C(4) | 115.9(13) | O(14)–C(13)–C(14) | 112.6(17) |
| C(3)–C(4)–O(6) | 123.1(17) | C(13)–C(14)–O(16) | 117.1(21) |
| C(3)–C(4)–O(5) | 113.7(14) | C(13)–C(14)–O(15) | 116.6(17) |
| O(6)–C(4)–O(5) | 123.2(16) | O(16)–C(14)–O(15) | 126.2(18) |
| C(4)–O(5)–Sb(2) | 115.3(10) | C(14)–O(15)–Sb(2) | 114.5(12) |

bond distances are 1.97, 2.00, 1.99, and 2.01 Å. This correlates well with electron diffraction studies of $PF_3Cl_2$,[18] $CH_3PF_4$, and $(CH_3)_2PF_3$,[19] for example, in which there is bond lengthening in the axial direction and in which the more electronegative substituents (fluorine atoms) are in axial positions. Bond lengthening in the axial direction, an average 0.17 Å in the potassium antimony tartrate structure, also correlates well with an average 0.24 Å lengthening of the antimony–halide bond in the axial direction in antimony halide structures determined in this laboratory.[20] In such molecules the best bonding description is to neglect *d*-orbitals in the first approximation and use primarily *p*-orbitals for bonding the longer bonds being three-center four-electron bonds.[19]

Between tartrato-(4)-bridged binuclear anions there appear to be some electrostatic interaction with two antimony–oxygen interatomic distances shorter than the sum of the van der Waal radii, 3.60 Å.[21] These are Sb(1)–O(13$^{ii}$) and Sb(2)–O(6$^{vi}$), 2.97 and 3.35 Å respectively. These interactions are probably important only in the solid state.

Water molecules very often play a very important role in crystalline inorganic hydrated salts as ligands for metal ions and to minimize repulsion between anions.[22] The three water molecules in the potassium antimony tartrate structure are hydrogen bonded to one another as O(W1)–O(W2)–O(W3) chains, and are hydrogen bonded to tartrate oxygen atoms in different antimony tartrate dimers related by the c-centering operation (Figure 4). These hydrogen bonds, O(W1)–H(W1a) $\cdots$O(13)($^1/_2$+x, $-^1/_2$+y, z), O(W1)–H(W1b)$\cdots$ O(16), O(W2)–H(W2b)$\cdots$O(3)($-^1/_2$ + x, $-^1/_2$ + y, z), O(W3)–H(W3a)$\cdots$O(15), connect the antimony tartrate dimers in infinite sheets parallel to the a–b plane,

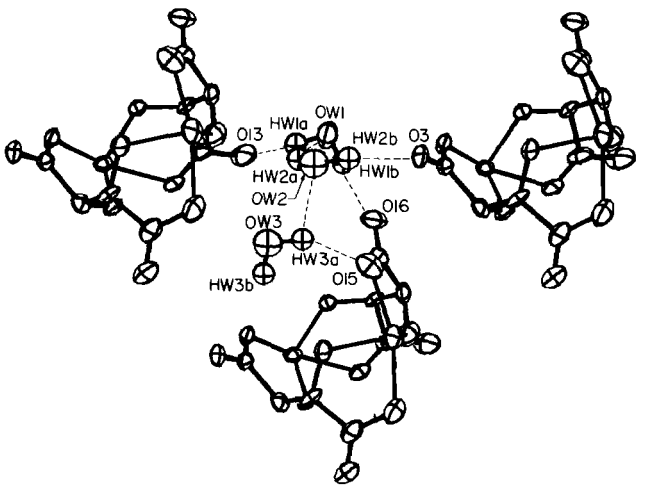


Figure 4. View displaying the hydrogen–bonding of water molecules between antimony–tartrate dimers.

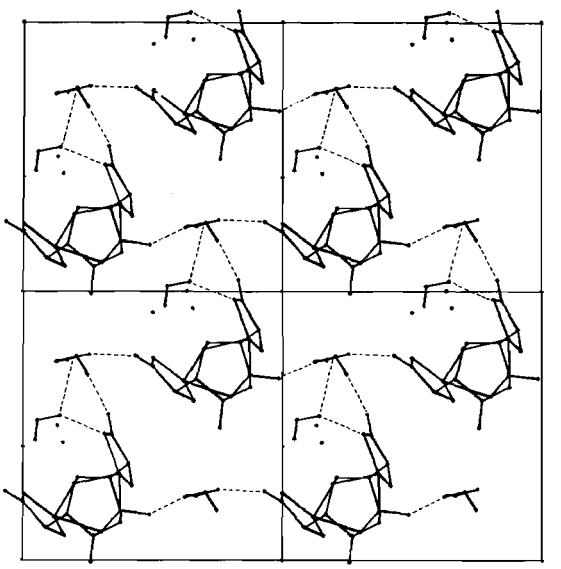

Figure 5. Intermolecular packing diagram showing the hydrogen bonding network. This is a projection onto the a–b plane of four quarter-unit cell contents with $0 \leq z \leq 0 \cdot 25$. There are four hydrogen-bonded infinite sheets for $0 \leq z \leq 1 \cdot 0$.

as seen in Figure 5. The hydrogen bonding distances and angles are given in Table V.

The potassium atoms are situated between these layers and stabilize the solid *via* electrostatic interactions with tartrate and water oxygen atoms. Potassium–$H_2O$ oxygen distances O(W1)–K(3$^{vi}$), O(W3)–K(2$^{vi}$), and O(W3)–K(3$^{iv}$): 2.76, 3.15, and 2.68 Å, respectively, are comparable to K–O($H_2O$) distances in K(Au(CN)$_4$) $\cdot H_2O$[23] and K($B_5O_6$(OH)$_4$)$\cdot 2H_2O$.[24] In addition, there are antimony–$H_2O$ oxygen interactions, O(W2)–Sb(2$^{vi}$) and O(W2)–Sb(2$^{vii}$), 3.26 and 3.47 Å, respectively. The latter distances are somewhat less than the sum of the van der Waal radii, 4.0 Å,[21] and remind one of the Reihlen and Hezel structure where water occupies an antimony coordination site, but it is doubtful that this weak interaction would cause the water molecule to ionize in solution.

The coordination geometry of water oxygen atoms is not as clearly defined as in many other inorganic hydrate structures,[25] where lone pair orbitals or the bisectrix of lone pair orbitals are directed toward metal atoms or are acceptors in hydrogen bonds. The potassium ions, in particular, do not necessarily occupy $sp^3$ coordination sites on the $H_2O$ oxygen atoms. O(W1), in addition to the two bonding atoms H(W1a) and H(W1b), is coordinated to K(3) and is also the acceptor atom in a hydrogen bond to O(W2). O(W2) is the donor atom in two hydrogen bonds and is the acceptor atom in a hydrogen bond with O(W3). It is also weakly coordinated to Sb(2$^{vi}$) and Sb(2$^{vii}$). The third water molecule, O(W3), is coordinated to two potassium ions K(2$^{vi}$) and K(3$^{iv}$). Only one hydrogen atom in the

TABLE V. Interatomic distances and angles involving water molecules.[a]

(a) Selected Distances (Å) and Angles (deg)

| | |
|---|---|
| O(W1)–H(W1a) | 0.95 |
| O(W1)–H(W1b) | 0.94 |
| O(W2)–H(W2a) | 0.83 |
| O(W2)–H(W2b) | 1.06 |
| O(W3)–H(W3a) | 1.04 |
| O(W3)–H(W3b) | 0.90 |
| H(W1a)–O(W1)–H(W1b) | 105 |
| H(W2a)–O(W2)–H(W2b) | 143 |
| H(W3a)–O(W3)–H(W3b) | 102 |
| O(W1)–O(16) | 2.89(2) |
| O(W1)–O(W2) | 2.90(4) |
| O(W1)–O($13^{vii}$)[b] | 3.04(2) |
| O(W1)–K($3^{vi}$) | 2.76(2) |
| O(W2)–O($3^{xi}$) | 2.93(4) |
| O(W2)–O($5^{vi}$) | 3.10(4) |
| O(W2)–O($6^{x}$) | 3.20(4) |
| O(W2)–O($14^{vii}$) | 3.24(4) |
| O(W2)–Sb($2^{vi}$) | 3.26(3) |
| O(W2)–Sb($2^{vii}$) | 3.47(3) |
| O(W3)–O(14) | 2.96(4) |
| O(W3)–O($5^{vii}$) | 3.00(4) |
| O(W3)–O(W2) | 3.14(5) |
| O(W3)–K($2^{vi}$) | 3.15(3) |
| O(W3)–K($3^{iv}$) | 2.68(3) |

(b) Hydrogen Bonding Distances (Å) and Angles (deg)

| Donor | Hydrogen | Acceptor | Distances | | | O–H···O angle |
|---|---|---|---|---|---|---|
| | | | O–O | O–H | H···O | |
| O(W1) | H(W1a) | O($13^{vii}$) | 3.04(2) | 0.95 | 2.42 | 121 |
| O(W1) | H(W1b) | O(16) | 2.89(2) | 0.94 | 1.95 | 172 |
| O(W2) | H(W2a) | O(W1) | 2.90(4) | 0.83 | 2.31 | 129 |
| O(W2) | H(W2b) | O($3^{xi}$) | 2.93(4) | 1.06 | 2.07 | 137 |
| O(W3) | H(W3a) | O(15) | 2.96(4) | 1.04 | 2.06 | 144 |
| O(W3) | H(W3a) | O(W2) | 3.14(5) | 0.90 | 2.60 | 112 |

[a] The hydrogen atom positions are estimated from the neutron Fourier synthesis. [b] The superscripts used in this table and in the text refer to the following transformations:

| | | | | | | | |
|---|---|---|---|---|---|---|---|
| i: | x, | −y, | −z | vi: | $^1/_2$−x, | $-^1/_2$+y, | $^1/_2$−z |
| ii: | $^1/_2$+x, | $^1/_2$−y, | −z | vii: | $^1/_2$+x, | $-^1/_2$+y, | z |
| iii: | −x, | y, | $^1/_2$−z | viii: | $-^1/_2$+x, | $^1/_2$+y, | z |
| iv: | 1−x, | y, | $^1/_2$−z | ix: | $-^1/_2$−x, | $-^1/_2$−y, | $-^1/_2$+z |
| v: | $^1/_2$−x, | $^1/_2$+y, | $^1/_2$−z | x: | x, | −1+y, | z |
| | | | | xi: | $-^1/_2$+x, | $-^1/_2$+y, | z |

third water molecule appears to be involved in hydrogen bonding, with bifurcated hydrogen bonds O(W3)–H(W3a)···O(11) and O(W3)–H(W3a)···O(W2).

## References


1 B. Kamenar, D. Grdenić, and C.K. Prout, *Acta Cryst., B26,* 181 (1970).
2 G.A. Kiosse, N.I. Golovastikov, A.V. Ablov, and N.V. Belov, *Doklady Akad. Nauk. SSSR, 177,* 329 (1967) [*Soviet Physics-Doklady, 12,* 990 (1968)].
3 Hsiang–Ch'i Mu, *K'o Hseuh T'ung Pao, 17,* 502 (1966).
4 H. Reihlen and E. Hezel, *Ann. Chem., 487,* 213 (1931).
5 G.A. Kiosse, N.I. Golovastikov, and N.V. Belov, *Kristallografiya, 9,* 402 (1964) [*Soviet Physics – Crystallographie, 9,* 321 (1964)].
6 R.C. Weast, Ed., "Handbook of Chemistry and Physics," Chemical Rubber Co., Cleveland, Ohio, 1970, p. B–121.
7 L.E. Alexander and G.S. Smith, *Acta Cryst., 15,* 983 (1962).
8 S.L. Lawton and R.A. Jacobson, *Inorg. Chem., 7,* 2124 (1968).
9 C.R. Hubbard, C.O. Quicksall, and R.A. Jacobson, *Acta Cryst., A28,* 236 (1972).

10 C.R. Hubbard, C.O. Quicksall, and R.A. Jacobson, *Acta Cryst.,* in press.

11 G.E. Bacon, "Neutron Diffraction," Oxford Univ. Press, Oxford, 1962, pp. 31, 61.

12 In addition to OR FLS, the authors wish to acknowledge the use of OR FFE (Busing, Martin, and Levy), OR TEP (C.K. Johnson), and LSP, a least squares plane program by D.E. Williams.

13 P.A. Doyle and P.S. Turner, *Acta Cryst., A24,* 390 (1968).

14 "International Tables for X-ray Crystallography," Vol. III, 2nd Ed., Kynoch Press, Birmingham, England, 1968, p. 215.

15 Neutron Diffraction Commission, *Acta Cryst., A25,* 391 (1969).

16 H.P. Hanson, F. Hermann, J.D. Lea, and S. Skillman, *Acta Cryst., 17,* 1040 (1964).

17 R.E. Tapscott, R.L. Belford, and I.C. Paul, *Coordin. Chem. Rev., 4,* 323 (1969).

18 J.E. Griffiths, R.P. Carter, Jr., and J.R. Holmes, *J. Chem. Phys., 41,* 863 (1964).

19 L.S. Bartell and K.W. Hansen, *Inorg. Chem., 4,* 1777 (1965).

20 D.R. Schroeder and R.A. Jacobson, *Inorg. Chem., 12,* 210 (1973), and references therein.

21 L. Pauling, "The Nature of the Chemical Bond," Cornell Univ. Press, Ithaca, N.Y., 1960, p. 260.

22 W.C. Hamilton and J.A. Ibers, "Hydrogen Bonding in Solids," Benjamin, New York, N.Y., 1968, p. 204.

23 C. Bertinotti and A. Bertinotti, *Acta Cryst., B26,* 422 (1970).

24 J.P. Ashmore and H.E. Petch, *Canad. J. Phys., 47,* 1091 (1969).

25 G. Ferraris and M. Franchini–Angela, *Acta Cryst., B28,* 3572 (1972).